Michl, A.; Weissmueller, J.; Mueller, S.:

Sign-inverted response of aluminum work function to tangential strain

In: Journal of Physics: Condensed Matter (2013) IOP

DOI: 10.1088/0953-8984/25/44/445012

Sign-inverted response of aluminium work function to tangential strain

A Michl[1,2], J Weissmüller[1,3] and S Müller[2]

[1]Institute of Materials Research, Materials Mechanics, Helmholtz-Zentrum Geesthacht, 21502 Geesthacht, Germany

[2]Institute of Advanced Ceramics, Hamburg University of Technology, 21073 Hamburg, Germany

[3]Institute of Materials Physics and Technology, Hamburg University of Technology, 21073 Hamburg, Germany

E-mail: `stefan.mueller@tuhh.de`

Abstract. We have investigated the response of the work function W of low-index aluminium surfaces to tangential strain by using first-principles calculations based on density functional theory. This response parameter is a central quantity in electrocapillary coupling of metal electrodes relating to the performance of porous metal actuators and surface stress based sensing devices. We find that Al surfaces exhibit a positive response for all orientations considered. By contrast, previous studies reported negative-valued response parameters for clean surfaces of several transition metals. We discuss separately the response of W to different types of strain and the impact of the strain on the Fermi energy and on the surface dipole. We argue that the reason for the abnormal positive sign of the Al response parameter lies in its high valence electron density.

PACS numbers: 68.35.Gy, 73.30.+y, 71.15.Mb, 68.47.De

Submitted to: *J. Phys.: Condens. Matter*

1. Introduction

The response of the surface stress f of a metallic surface to a variation in the superficial charge density q defines an electrocapillary coupling parameter, $\varsigma = \delta f/\delta q$, which is a fundamental materials parameter of solid surfaces. The surface-induced stresses in the bulk of a solid electrode result in an elastic deformation, thus allowing to determine ς from the bending of cantilevers [1, 2] or from porous metal expansion [3] in reaction to electric charging in electrolyte. This electrocapillary coupling strength is appreciable for nanoscale metal structures with a high surface-to-volume ratio, suggesting their use as actuators with large stroke and strain energy density [3, 4, 5].

Studies of the electrocapillary coupling go back to work by A. Y. Gokhshtein in the 1960's and 70's [6, 7, 8]. He was the first to point out a thermodynamic Maxwell relation, $\varsigma = \mathrm{d}f/\mathrm{d}q|_e = \mathrm{d}U/\mathrm{d}e|_q$, that links the surface stress charge response at equilibrium to the response of the electrode potential U to tangential strain e. More recently, the issue received renewed attention after careful measurements of $\mathrm{d}f/\mathrm{d}q$ by Haiss and co-workers, indicating a link to charge transfer during anion adsorption [2, 9]. Moreover, the impact of strain on the electronic structure and hence on adsorption energies and energy barriers provides a means to tune the catalytic activity of metal surfaces [10, 11, 12]. Tabard-Cossa *et al.* [13] and Smetanin *et al.* [14] used dilute and weakly adsorbing electrolytes in order to study the intrinsic response of the metal surface without specific adsorption. Their response parameter of $\mathrm{d}f/\mathrm{d}q = -2.0 \pm 0.1$ V for a (111)-textured Au electrode agrees well with a subsequent measurement of $\mathrm{d}U/\mathrm{d}e = -1.83 \pm 0.1$ V, thus confirming the Maxwell relation experimentally [15].

Since the variation of the potential of zero charge of an electrode surface in electrolyte is closely linked to the variation of the work function W in vacuum [16, 17], it is possible to investigate electrocapillary coupling using the concepts and methods of theoretical surface science without explicit consideration of the electrolyte solution [18]. Relating the coupling coefficient of the work function $\varsigma_W := \mathrm{d}W/\mathrm{d}e$ to the surface stress charge coefficient via $\varsigma = q_0^{-1}\varsigma_W$ ‡ with q_0 the elementary charge, Umeno *et al.* [18] obtained a value of $\varsigma = -1.86 \pm 0.016$ V from density functional theory (DFT) calculations of Au(111) surfaces in vacuum. This is indeed very similar to the experimental results for the coupling coefficient [14, 15].

Over the past decade, quantitative data related to electrocapillary coupling has been accumulated for a number of clean metal surfaces – notably of transition metals – from both experimental determination of $\mathrm{d}f/\mathrm{d}q$ [14, 19, 20, 21] and $\mathrm{d}U/\mathrm{d}e$ [15] as well as from first-principles calculations of the work function strain response [18, 22, 23]. In spite of the increasing interest in electrocapillary coupling, both from experiment and from theory, there is no satisfactory picture of the underlying mechanisms that would allow to predict ς for a given materials surface as of yet.

Nonetheless, previous studies have identified important trends and contributed to the understanding of electrocapillary coupling. The negative sign of the coupling coefficients for the transition metals has been rationalized by a phenomenological model explaining the surface stress variation as the transverse contraction in response to charge-induced relaxation [24]. A parabolic variation of the magnitude of ς with the d-band occupancy for the 4d metals has been attributed to the occupation of bonding or antibonding orbitals by excess charge [23]. From

‡ This is merely the combination of (5) and (6) of [18] adapted to our notation.

the perspective of the work function strain response, the negative sign has been rationalized by an increase in the surface dipole due to the increased spill out of electronic charge at the compressed surface [18, 22]. Another qualitative argument for the negative sign is given in [9, 21, 25] which is based on the electron density dependence of the work function in the jellium model. However, quantitatively, the jellium estimates did not match the experimental data in the case of Au.

While the quantitative failure of the jellium model for a d-metal like Au is not surprising due to the contributions from directional bonding, jellium is considered a suitable model system for free-electron-like metals. One may thus expect that the response behaviour of a simple sp-bonded metal like aluminium should be well established qualitatively as well as quantitatively. However, the results reported in the literature do not even agree with respect to the sign of the response (see e.g. [26, 27] and reference therein). For example, Kiejna and Pogosov [28] and Pogosov and Kurbatsky [29] have found a decrease of the work function in response to a uniaxial tensile strain using a modified stabilized jellium model, whereas Levitin and Loskutov [26] report positive values from theoretical calculations using different variants of the jellium model as well as from experimental determination of the variation of the work function with elastic deformation.

In this paper, we evaluate the strain response of the work function of low-index aluminium surfaces from first principles using density functional theory. This method has proven its ability to determine electrocapillary coupling coefficients in close agreement to electrochemical experiments [18]. In contrast to the negative values reported for transition metals, we find positive response parameters for Al surfaces for all orientations considered. In order to explore reasons for this unusual positive sign, we analyze trends of the strain response of the work function and its components with varying electron density within the jellium model. An increasing trend of the jellium response with increasing electron density is found, which suggests that the high valence electron density of aluminium is responsible for the sign-inversion for the electrocapillary response.

The paper is organized as follows: Section 2 contains computational details and a compilation of the different strain situations. In Section 3 we present results for the work function strain response parameters of aluminium surfaces in (100), (111) and (110) orientation for different types of strain and analyze their contributions. A discussion of the results leading to a possible explanation for the sign-inversion of the Al coupling coefficient is given in Section 4 followed by the conclusions in Section 5.

2. Methodology

2.1. Details of the DFT calculations

The calculations were performed using density functional theory as implemented in the plane-wave code VASP [30, 31, 32, 33]. PAW [34, 35] potentials were used to treat the interaction between valence electrons and the ion cores and the electronic wave functions were expanded using a 400 eV cutoff. Methfessel-Paxton [36] smearing with a smearing width of 0.2 eV was employed. For the exchange-correlation functional the parametrization by Perdew, Burke and Ernzerhof [37] was chosen. Additional calculations with different exchange-correlation functionals (PW91 [38] and LDA [39]) have yielded similar results demonstrating that the sign-inversion of $\mathrm{d}W/\mathrm{d}e$ for Al is not an artefact of a particular functional. Surfaces were modelled

by symmetric slabs in the respective orientation containing one atom per layer separated by a vacuum region, which is at least 16 Å wide (in the unstrained state). It turned out that an accurate determination of the aluminium work function requires a rather fine k-point grid and in particular an exceptionally high number of layers. More details on the convergence properties and results for the different exchange-correlation functionals are available as Supplementary Data. The results presented in the following sections were all obtained with well-converged Monkhorst-Pack [40] grids of 41×41×1 k-points for the (100) and (111) surface and analogously 41×29×1 k-points for the (110) surface as well as very thick slabs with 41 layers for the (100) surface, 37 for (111) and 63 for (110).

We reference all energies and potentials to the average electrostatic potential in the bulk region of the slab $\bar{V}_{\mathrm{bulk}}$. This quantity is obtained by performing a macroscopic average [41] over the electrostatic potential as implemented in the post-processing routines of the Quantum ESPRESSO package [42]. Using this convention, we can calculate the work function as the difference between its physical components, the dipole barrier $V_{\mathrm{dip}} = V_{\mathrm{vac}} - \bar{V}_{\mathrm{bulk}}$ (where V_{vac} is the vacuum level) and the Fermi energy E_{f} (with reference to the average bulk potential). In other words,

$$W = V_{\mathrm{dip}} - E_{\mathrm{f}}, \tag{1}$$

which is illustrated in figure 1. Fall *et al.* [41] have suggested to determine E_{f} from a separate bulk calculation in order to avoid quantum size effects. For the thickest slabs used in this work the Fermi energies obtained from the surface calculations agree to within 3 meV with the bulk Fermi energy.

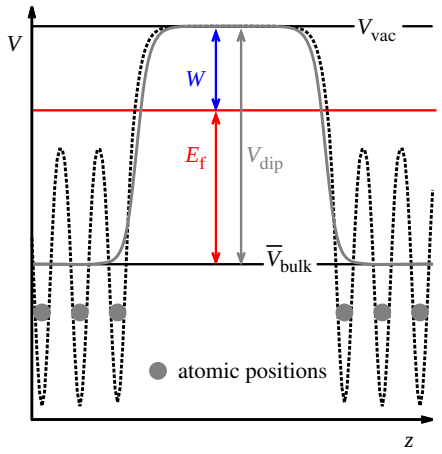

Figure 1. Illustration of the calculation of the work function with (1). The black dashed curve is the plane averaged electrostatic potential of the slab. From the macroscopically averaged electrostatic potential (grey solid curve) the dipole barrier V_{dip} is obtained as the difference between the vacuum potential V_{vac} and the average bulk potential $\bar{V}_{\mathrm{bulk}}$.

2.2. Implementing strain

The stress-free lattice parameter, a_0, was determined from bulk calculations via a Murnaghan fit as $a_0 = 4.040$ Å. All strain values in this work are referred to the cubic crystal lattice at this value of the lattice parameter.

In order to obtain the reference configuration of the slabs with a given orientation and layer number we constructed the slabs as truncated bulk crystals and allowed the first 10 surface layers on each side to relax until the forces were below 0.005 eV/Å. This relaxed equilibrium structure was used as the starting point for all further calculations.

The different components of the deformation of the strained surface slabs are illustrated in figure 2. For the evaluation of the work function strain response parameter $\varsigma_W = \mathrm{d}W/\mathrm{d}e$, the surface slab was subjected to isotropic in-plane strain. Since the strain parameter $e = \delta A/A_0$ (with A_0 the area of the two-dimensional surface unit cell of the unstrained slab) measures the relative change in surface area A, this corresponds to scaling both in-plane lattice vectors by a factor of $\sqrt{1+e}$. Strain values of up to $|e| = 0.04$ were considered, which is expected to be small enough to yield an approximately linear relation between W and e. The coupling coefficient can then be obtained as the slope of a linear fit.

The interlayer distances of the new equilibrium configuration for a given in-plane strain will differ from those of the unstrained reference configuration, when no external forces are applied in the normal direction (which is the typical boundary condition in experimental studies). This is related firstly to the transverse contraction tendency of the material and secondly to a possible change in the surface relaxation behaviour in response to strain. Thus the strain dependence of the work function is contained in the expression

$$W = W^{\mathrm{h}}(e, E_\perp) + \Delta W^{\mathrm{rel}}(e, E_\perp), \tag{2}$$

where the strain parameters are the applied in-plane strain e and the normal strain $E_\perp$ corresponding to the scaling of each interlayer distance $d_{i,i+1}$ by the identical factor $1 + E_\perp$. $\Delta W^{\mathrm{rel}}(e, E_\perp)$ accounts for the change in the work function due to surface relaxations different from those of the unstrained reference configuration and corresponds to the difference between W and the work function of a homogeneously strained surface slab $W^{\mathrm{h}} = W^{\mathrm{h}}(e, E_\perp)$.

For this homogeneous deformation, in-plane strain was imposed and all interlayer distances were scaled uniformly according to the transverse contraction tendency. In order to determine the equilibrium bulk interlayer distance for a given in-plane strain and hence the corresponding scaling factor we considered bulk unit cells in the same orientation as the respective surface (i.e. having the same in-plane lattice vectors). For each e we performed a series of calculations for varying bulk interlayer distances d (corresponding to varying $E_\perp$). The equilibrium bulk layer spacing d_0^e for a given in-plane strain e is then obtained from a quadratic fit of the total energy vs. d curve. The transverse contraction tendency for a surface in hkl orientation is quantified by the parameter τ_{hkl}, which was extracted from a linear fit to the graph of $E_\perp$ vs. e. We find τ_{hkl} largest for the (100) surface ($\tau_{100} = 0.54$), whereas similar values are obtained for (111) and (110) orientation ($\tau_{111} = 0.45$ and $\tau_{110} = 0.48$).

The strain response parameter of the work function derived from these homogeneously deformed slabs is denoted as $\mathrm{d}W/\mathrm{d}e|^{\mathrm{scaled}}$. In order to gain further insight, we decompose this response parameter according to the different components of the deformation and inspect the variation of the work function with each of the parameters e and $E_\perp$ separately. This decomposition can be written as

$$\begin{aligned} \left.\frac{\mathrm{d}W}{\mathrm{d}e}\right|^{\mathrm{scaled}} &= \left.\frac{\partial W^{\mathrm{h}}}{\partial e}\right|_{E_\perp} + \left.\frac{\partial W^{\mathrm{h}}}{\partial E_\perp}\right|_{e} \frac{\mathrm{d}E_\perp}{\mathrm{d}e} \\ &= \left.\frac{\partial W^{\mathrm{h}}}{\partial e}\right|_{E_\perp} - \tau_{hkl} \left.\frac{\partial W^{\mathrm{h}}}{\partial E_\perp}\right|_{e}, \end{aligned} \tag{3}$$

where $\partial W^{\mathrm{h}}/\partial e$ is the response to in-plane strain with fixed layer distances and $\partial W^{\mathrm{h}}/\partial E_{\perp}$ to uniaxial strain in the direction perpendicular to the surface with fixed in-plane lattice vectors.

The response parameter $\varsigma_W = \mathrm{d}W/\mathrm{d}e$ corresponding to the experimental situation was then determined by starting from a laterally strained "scaled" configuration and allowing for relaxation of the outermost 10 layers on each side, using again a force convergence threshold of 0.005 eV/Å. The geometries obtained in this way remain almost unchanged when also the remaining (bulk) layers are free to relax. The corresponding changes in the strain response parameters $\mathrm{d}W/\mathrm{d}e$ are on the order of 0.1% and hence negligible, which justifies our approach. $\mathrm{d}W/\mathrm{d}e$ can thus be taken as the total strain response for (fully) relaxed layer distances.

Apart from an obvious saving in computer time our procedure (scaling plus relaxation of the surface layers only) has moreover the advantage that the dipole barrier can be accurately determined by the macroscopic averaging technique.

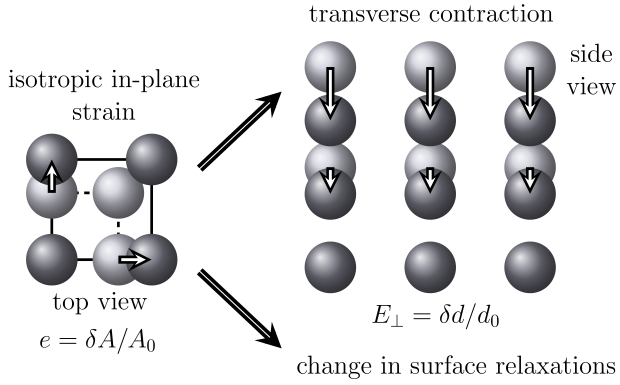

Figure 2. Illustration of the strain components for the example of a (100) surface of a cubic crystal. As a consequence of the isotropic in-plane strain the interlayer distances change due to transverse contraction and a potentially different surface relaxation behaviour.

Table 1. Compilation of the different coupling coefficients between work function and strain considered in this work. The response parameter relevant for comparison to experiment is marked in bold.

response	description
$\partial W^{\mathrm{h}}/\partial e$	in-plane strain with fixed layer distances
$\partial W^{\mathrm{h}}/\partial E_{\perp}$	uniaxial strain perpendicular to the surface
$\mathrm{d}W/\mathrm{d}e\vert^{\mathrm{scaled}}$	in-plane strain with scaled layer distances
$\mathbf{d}\boldsymbol{W}/\mathbf{d}\boldsymbol{e}$	in-plane strain with relaxed layer distances

Table 1 summarizes the various response parameters that are considered in this work. The coupling coefficient corresponding to relaxed interlayer distances, which is the relevant quantity for comparison to experiment, is marked in bold.

3. Results

3.1. Work function strain response parameters

Before discussing the behaviour of the work function in response to different types of strain we show established properties of the unstrained aluminium surfaces, which are also of interest in

the context of the present study, and compare them to literature values (see table 2).

The top layer relaxation,

$$\Delta d_{12} = \frac{d_{1,2} - d_0}{d_0}\,, \tag{4}$$

quantifies the change in the interlayer spacing between the first and second layer $d_{1,2}$ with respect to the equilibrium layer distance d_0 (which amounts to $a_0/2$ for Al(100), $a_0/\sqrt{3}$ for (111) and $a_0/(2\sqrt{2})$ for (110)). While the (110) surface shows a significant inward relaxation of the first layer by more than 7 % consistent with the electrostatic model by Finnis and Heine [43], the (100) and (111) surfaces exhibit an anomalous outward relaxation of about 1 %.

Table 2. Surface energies γ, top layer relaxations Δd_{12} and work functions W for the three surface orientations as obtained in this work along with theoretical results from [44] and experimental values from [45], [46], [47] and [48].

	Al(100)	Al(111)	Al(110)
γ [eV/atom]	0.48	0.36	0.72
	0.48[a]	0.36[a]	0.72[a]
Δd_{12} [%]	1.5	1.0	−7.5
	2.0 ± 0.8[b]	1.3 ± 0.8[c]	-8.4 ± 0.8[d]
W [eV]	4.261	4.050	4.058
	4.41 ± 0.03[e]	4.24 ± 0.02[e]	4.28 ± 0.02[e]

[a] [44] [b] [45] [c] [46] [d] [47] [e] [48]

Table 3. Response of the work function to different types of strain and transverse contraction parameters τ_{hkl}.

		Al(100)	Al(111)	Al(110)
$\partial W^{\mathrm{h}}/\partial e$	[eV]	0.47	0.50	0.62
$\partial W^{\mathrm{h}}/\partial E_{\perp}$	[eV]	−1.22	−0.45	−0.18
$\mathrm{d}W/\mathrm{d}e\vert^{\mathrm{scaled}}$	[eV]	1.11	0.67	0.71
$\mathbf{d}\boldsymbol{W}/\mathbf{d}\boldsymbol{e}$	**[eV]**	**1.02**	**0.63**	**0.58**
τ_{hkl}	[no units]	0.54	0.45	0.48

Although the surface stress was not calculated in this work, we note that aluminium has a tensile surface stress (see [49]), as generally expected for metal surfaces. In other words, it does not exhibit an anomalous sign of this quantity.

Al has, however, an anomaly concerning the face-dependence of the work function. Unlike other fcc metals, it has the highest work function in the (100) orientation and not in the most close-packed (111) orientation as would be expected from Smoluchowski's rule [50]. Fall *et al.* [41] attributed this to the orientation dependent filling of the atomiclike p states at the surface. According to them, the charge transfer from the p-orbitals perpendicular to the surface to those parallel to the surface, which decreases the surface dipole, is most pronounced for the (111) surface.

We now show the results for the response of the work function of aluminium surfaces to different types of strain. The values for the various response parameters are listed in table 3. We start out with the Al(100) surface, where for the case of interlayer distances fixed at the

values for the (relaxed) unstrained surface we get $\partial W^{\mathrm{h}}/\partial e = 0.47$ eV (see circles in figure 3(a)). Taking into account the transverse contraction tendency by scaling of the interlayer distances a larger response of $\mathrm{d}W/\mathrm{d}e|^{\mathrm{scaled}} = 1.11$ eV is obtained. The sensitivity of the coupling coefficient on the interlayer distances is reflected in the relatively large response parameter to uniaxial strain perpendicular to the surface $\partial W^{\mathrm{h}}/\partial E_{\perp} = -1.22$ (see triangles in figure 3(a)). The negative sign is responsible for the observed order $\mathrm{d}W/\mathrm{d}e|^{\mathrm{scaled}} > \partial W^{\mathrm{h}}/\partial e$. The total response including surface relaxations is with $\mathrm{d}W/\mathrm{d}e = 1.02$ eV (see squares in figure 3(a)) of similar magnitude as for scaled layer distances.

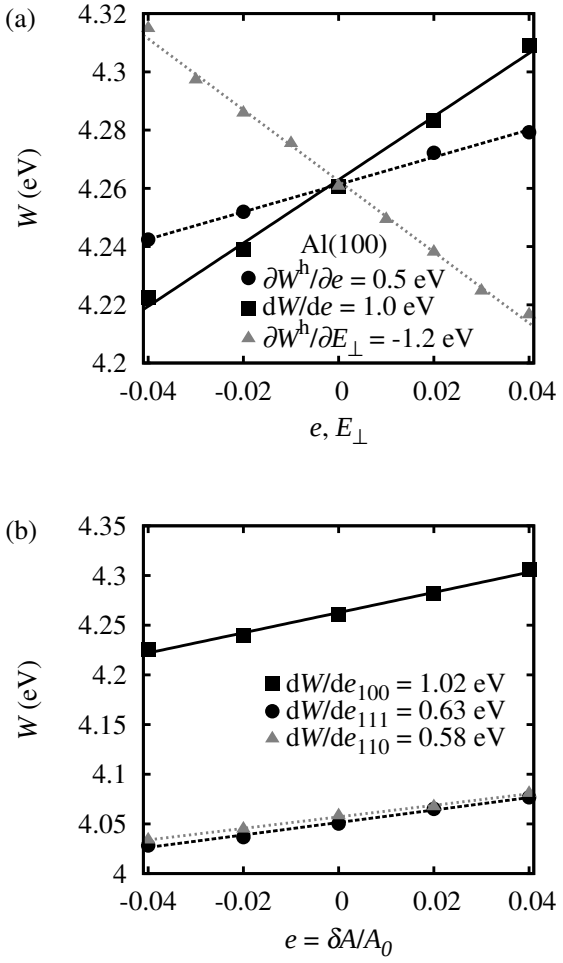

Figure 3. Work function vs. strain for the Al(100) surface in different strain situations (a) and for in-plane strain with relaxed interlayer distances for different orientations (b).

A comparison of the three surface orientations is shown in figure 3(b), where the work function for relaxed layers is plotted as a function of the in-plane strain. The response for the (100) surface is the largest one ($\mathrm{d}W/\mathrm{d}e_{100} = 1.02$ eV), whereas the magnitude is similar for the other two orientations ($\mathrm{d}W/\mathrm{d}e_{111} = 0.63$ eV and $\mathrm{d}W/\mathrm{d}e_{110} = 0.58$ eV).

Interestingly, the response parameters of all three surfaces are positive-valued. Positive response parameters have been reported for surfaces of palladium, platinum and gold when covered by a chemisorbed oxygen monolayer [21, 51, 52]. However, the finding of a positive-valued ς is in contrast to previous studies – in experiment [9, 15, 21, 51, 52] and theory [18, 23] – of clean surfaces of transition metals, which invariably found $\varsigma < 0$.

For all orientations the response to in-plane strain with fixed layer distances is rather similar (with values ranging from 0.47 eV to 0.62 eV). However, there is a large spread for the response to uniaxial strain perpendicular to the surface plane, which – together with the comparable magnitude of the transverse contraction parameters τ_{hkl} – leads eventually to a different total response parameter $\mathrm{d}W/\mathrm{d}e$.

3.2. Impact of surface relaxations

While for the (100) and (111) surface the scaling of the interlayer distances leads to a good approximation for the total response parameter (deviation between $\mathrm{d}W/\mathrm{d}e|^{\mathrm{scaled}}$ and $\mathrm{d}W/\mathrm{d}e$ of 9% and 7%, respectively), the values differ by more than 20% for the (110) surface. This can be ascribed to a different surface relaxation behaviour for the strained slabs. In figure 4 the interlayer distances $d_{i,i+1}$ for all three surface orientations for several tangential strain values e for relaxed layers and scaled layer distances are compared. For the (100) and (111) surfaces there are only small differences between scaled and relaxed layer distances. The minor change of surface relaxations with strain for those close-packed surface orientations is reflected in the good agreement between $\mathrm{d}W/\mathrm{d}e|^{\mathrm{scaled}}$ and $\mathrm{d}W/\mathrm{d}e$. For the more open (110) surface, however, significant modifications in the surface relaxations in consequence to strain are observed. While the spread of the first to second layer distances $d_{1,2}$ with strain is larger than obtained by on overall scaling according to the transverse contraction tendency, the second to third layer distance $d_{2,3}$ remains fixed at the value of the unstrained surface irrespective of the strain.

3.3. Anisotropy for the (110) surface

Although in principle the response has to be described by a two-dimensional tensor, for the isotropic (100) and (111) surfaces, the work function strain response parameter depends only on the change of the surface area and not on the direction of the in-plane strain. This can be understood most conveniently by considering the Maxwell relation $\mathrm{d}U/\mathrm{d}e|_q = \mathrm{d}f/\mathrm{d}q|_e$ mentioned in Section 1. The symmetry of the surface is reflected in the surface stress f, such that $\mathrm{d}f/\mathrm{d}q$ must be isotropic and hence by the Maxwell relation also $\mathrm{d}U/\mathrm{d}e$ and ς_W. The diagonal entries of the response parameter tensor $\hat{\varsigma_W}$ are thus identical: $[\hat{\varsigma_W}]_{xx} = [\hat{\varsigma_W}]_{yy} = \varsigma_W$. The situation is different, however, for the anisotropic (110) surface, where this symmetry argument does not hold and the diagonal entries can well be different. The scalar response parameter for the isotropic strain considered above is then the mean value of these entries $\varsigma_W = 1/2([\hat{\varsigma_W}]_{xx} + [\hat{\varsigma_W}]_{yy})$.

We have evaluated $[\hat{\varsigma_W}]_{xx}$ and $[\hat{\varsigma_W}]_{yy}$ for the (110) surface by imposing uniaxial strains in the surface plane while allowing for relaxation normal to the surface. The in-plane strain was either along the x- or the y-direction, with "x" referring to the direction parallel to the dense-packed rows of atoms (interatomic distances in the surface plane $a/\sqrt{2}$) and "y" to the direction normal to the rows (interatomic distances in the surface plane a). As can be seen in figure 5 basically all of the response comes from the strain in the more close-packed x-direction ($[\hat{\varsigma_W}]_{xx} = 1.13$ eV), whereas straining along the open y-direction has a negligible effect on the work function ($[\hat{\varsigma_W}]_{yy} = 0.02$ eV).

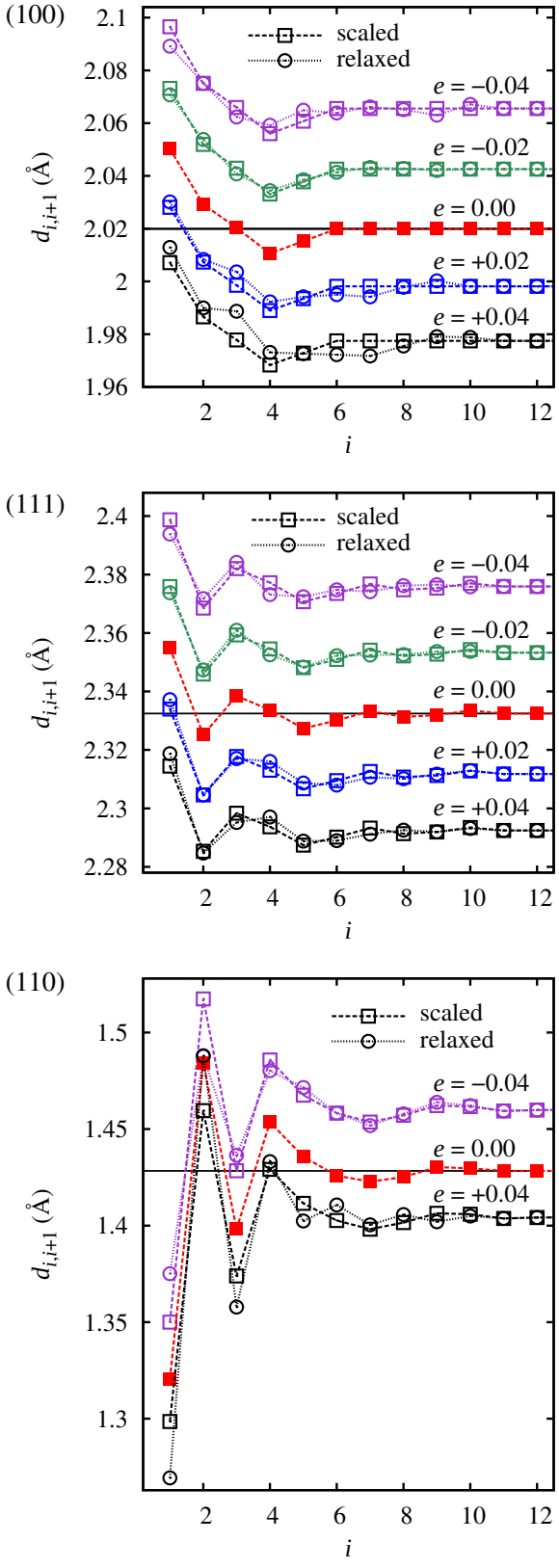

Figure 4. Interlayer spacings $d_{i,i+1}$ for the first 12 layers of Al (100), (111) and (110) surface slabs for different in-plane strains with scaled (squares) and relaxed (circles) interlayer distances. Filled symbols are used for the unstrained surfaces. The solid horizontal lines mark the equilibrium bulk layer spacing. For the (110) surface the graphs for $e = \pm 0.02$ have been left for the sake of visibility.

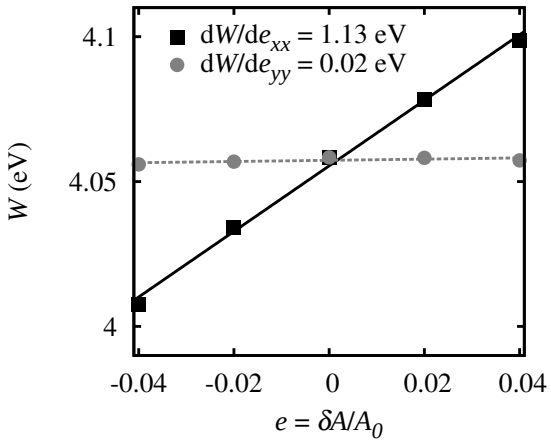

Figure 5. Response of the work function of Al(110) to uniaxial in-plane strain along x- (squares) and y-direction (circles) with linear fit.

3.4. Separating surface and volume contributions

As implied by (1) the work function can be decomposed into an orientation dependent surface quantity, the dipole barrier V_{dip}, which arises from the redistribution of the electronic charge at the metallic surface and a volume dependent quantity, the Fermi energy E_{f}. The total work function strain response $\mathrm{d}W/\mathrm{d}e$ then also splits into a surface and a volume contribution

$$\frac{\mathrm{d}W}{\mathrm{d}e} = \underbrace{\frac{\mathrm{d}V_{\mathrm{dip}}}{\mathrm{d}e}}_{\text{surface contribution}} - \underbrace{\frac{\mathrm{d}E_{\mathrm{f}}}{\mathrm{d}\varepsilon_{\mathcal{V}}}\frac{\mathrm{d}\varepsilon_{\mathcal{V}}}{\mathrm{d}e}}_{\text{volume contribution}} . \tag{5}$$

Table 4. Response of the dipole potential to different types of strain and response of the Fermi energy to volume strain $\varepsilon_{\mathcal{V}}$.

		Al(bulk)	Al(100)	Al(111)	Al(110)
$\partial V^{\mathrm{h}}_{\mathrm{dip}}/\partial e$	[eV]		−10.05	−9.99	−9.93
$\partial V^{\mathrm{h}}_{\mathrm{dip}}/\partial E_{\perp}$	[eV]		−11.78	−11.05	−10.73
$\mathrm{d}V_{\mathrm{dip}}/\mathrm{d}e$	[eV]		−3.67	−5.17	−4.78
$\mathrm{d}E_{\mathrm{f}}/\mathrm{d}\varepsilon_{\mathcal{V}}$	[eV]	-10.54			

The surface contribution depends on the magnitude as well as on the direction of the strain. Thus, in addition to the total response $\mathrm{d}V_{\mathrm{dip}}/\mathrm{d}e$, we inspect separately the variation of V_{dip} with in-plane, $\partial V^{\mathrm{h}}_{\mathrm{dip}}/\partial e$, and with normal strain, $\partial V^{\mathrm{h}}_{\mathrm{dip}}/\partial E_{\perp}$, in the same way as for the work function. Due to symmetry reasons, the Fermi energy of cubic crystals such as Al depends on the strain exclusively through the change in the volume $\mathcal{V}$, quantified by $\varepsilon_{\mathcal{V}} = \Delta\mathcal{V}/\mathcal{V}_0$. Computation of isotropically strained bulk cells yields a linear variation of E_{f} with $\mathrm{d}E_{\mathrm{f}}/\mathrm{d}\varepsilon_{\mathcal{V}} = -10.54$ eV. The scaling factor in the part of (5) which refers to the bulk contribution to the work function change can be approximated by $\mathrm{d}\varepsilon_{\mathcal{V}}/\mathrm{d}e \approx (1 - \tau_{hkl})$.

The volume and surface contributions to the work function strain response are listed in table 4 for the different strain situations. In contrast to the resulting strain response of the work function, the contributions have negative sign and are considerably larger in magnitude,

especially for the static cases without transverse contraction. The positive coupling coefficient of the work function is thus the difference of larger negative surface and volume contributions, which only nearly cancel.

4. Discussion

Since strain affects the surface dipole as well as the Fermi energy, both variations have to be taken into account to understand the resulting response of the work function. For Al and also for Cu (100) [53] both terms are negative, so that the sign of their difference cannot be predicted reliably based on qualitative arguments alone. While for Cu(100) the resulting response of the work function becomes negative [53], we obtain positive coupling coefficients for the (100), (111) and (110) surfaces of Al from our first-principles calculations. Compared to experimental and theoretical studies of transition metals, a positive response parameter for a clean metal surface is a curious finding. In order to find an explanation for the sign-inversion in the sp-bonded metal aluminium we analyze trends of the work function strain response for varying electron density within the jellium model.

The main approximation underlying this model – distinguishing it from the DFT-PBE approach on which the calculations of Sec. III are based – consists of replacing the discrete ion cores by a homogeneous positive background charge which cancels the electronic charge. This means that the only parameter differentiating the elements is their average valence electron density ρ_0, which is usually expressed in terms of the dimensionless Wigner-Seitz radius r_s § defined by

$$\frac{4}{3}\pi r_\mathrm{s}^3 r_\mathrm{B}^3 = \rho_0^{-1}. \tag{6}$$

In the frame of the isotropic jellium model, we approximate the strain as a small variation of the Wigner-Seitz radius around the value for the chosen element in its stress-free state. Taking the jellium results of Lang and Kohn [54] as a starting point we derive trends for the strain dependence of the components and the corresponding work function. From the analytic equation for the Fermi energy given in [54] containing a kinetic energy term as well as an exchange-correlation term (within the local density approximation) we calculate the response to (isotropic) volume strain $\varepsilon_\mathcal{V}$ via

$$\frac{\mathrm{d}E_\mathrm{f}}{\mathrm{d}\varepsilon_\mathcal{V}} = \frac{\mathrm{d}E_\mathrm{f}}{\mathrm{d}r_\mathrm{s}}\frac{\mathrm{d}r_\mathrm{s}}{\mathrm{d}\varepsilon_\mathcal{V}} = \frac{r_\mathrm{s}}{3}\frac{\mathrm{d}E_\mathrm{f}}{\mathrm{d}r_\mathrm{s}}, \tag{7}$$

which is shown in figure 6 as a function of the Wigner-Seitz radius (solid curve). The plot hence displays the response parameters for different elements in the metallic range ($2 \leq r_\mathrm{s} \leq 6$). Since Al has a high electron density and hence a comparatively small Wigner-Seitz radius of $r_\mathrm{s} = 2.07$, it is situated close to the lower boundary of the r_s-axis. The response parameters $\mathrm{d}E_\mathrm{f}/\mathrm{d}\varepsilon_\mathcal{V}$ are negative except for very low densities ($r_\mathrm{s} > 5$). This response consists of a negative contribution from the kinetic term $\mathrm{d}E_\mathrm{f,kin}/\mathrm{d}\varepsilon_\mathcal{V}$ and a positive contribution from the exchange-correlation term $\mathrm{d}E_\mathrm{f,xc}/\mathrm{d}\varepsilon_\mathcal{V}$. The negative kinetic energy contribution to the variation of the Fermi energy for small r_s dominates over the smaller positive $\mathrm{d}E_\mathrm{f,xc}/\mathrm{d}\varepsilon_\mathcal{V}$ leading to a larger negative response parameter for high-density metals than for metals with lower electron densities. This is consistent with the large negative response found in our DFT-PBE calculations for Al (compare table 4).

§ We take r_s to be the dimensionless radius (in units of the Bohr radius, r_B) of a sphere containing one electron.

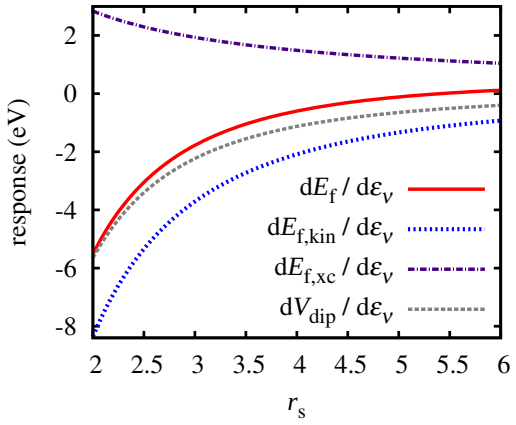

Figure 6. Contributions to the work function strain response in jellium model: response of Fermi energy E_f and dipole potential V_{dip} to volume strain ε_v as a function of the Wigner-Seitz radius r_s.

For obtaining the strain response of the dipole potential, we performed a fit ‖ to the self-consistent data points for V_{dip} of Lang and Kohn [54] and calculated the strain derivative analogously to (7). As can be seen in figure 6 the resulting strain response of the dipole potential (dashed curve) is of similar magnitude and shape as $dE_f/d\varepsilon_v$ over the whole r_s-range. As a consequence, their difference, the work function strain response, is considerably smaller than each term individually.

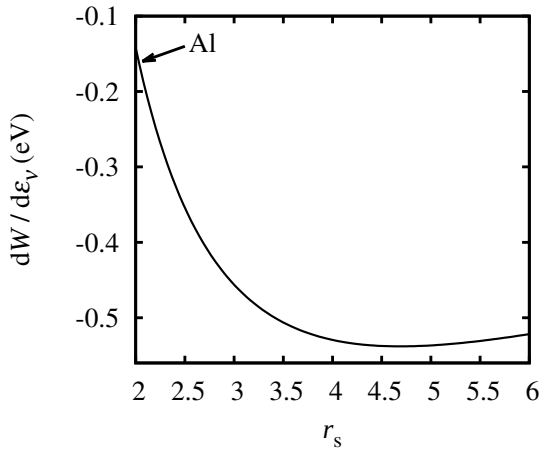

Figure 7. Response of the work function W to volume strain as a function of the Wigner-Seitz radius r_s in jellium model. The arrow denotes the position of aluminium.

Figure 7 shows the work function strain response of jellium plotted versus r_s. The response parameters are negative at any electron density in the metallic range, since the dipole contribution is not completely compensated by the Fermi energy term, which is also negative, but slightly smaller in magnitude (see figure 6). This is in agreement with the conclusions of [9, 21, 25] concerning the sign of the response parameter. However, our analysis reveals another interesting detail, which can provide a possible explanation for the unusual positive sign of the

‖ Best fit curve: $V_{dip} = 39.86\,\mathrm{eV}/r_s^2 - 6.34\,\mathrm{eV}/r_s$ with rms of 0.01.

DFT-PBE coupling coefficients for Al: The response parameters show an increasing trend with decreasing Wigner-Seitz radius r_s and hence with increasing valence electron density. Based on this trend of the jellium work function strain response for varying density, it can be concluded that – among the metals for which the jellium model is appropriate – Al as a high-density metal should have a large response parameter (see arrow in figure 7) While the jellium model still predicts a negative response, the trend is apparently shifted to positive values by applying the more quantitative DFT-PBE method.

We note that the curve in figure 7 was determined directly as the difference between the jellium response of V_{dip} and E_{f}. In addition, we have also tested direct fits to the work function data of Lang and Kohn with less parameters including a linear fit like in [9, 21, 25]. While the precise shape is somewhat dependent on this choice, the main feature of increasing response with increasing electron density remains present for all tested fit curves. Moreover, we have checked the persistence of this trend also for the stabilized jellium model [55, 56, 57], which removes some known pathological features of ordinary jellium. Using the data of Fiolhais and Perdew [58] for the work function of some simple metals, a similar increasing trend with increasing electron density is found for low r_s values.

5. Conclusions

We have evaluated the response of the work function of low-index aluminium surfaces to elastic strain from first principles. Our work is mainly centred on the response to tangential strain e at constant normal stress. This parameter is closely linked to the electrocapillary coupling parameter ς that governs the variations of electrode potential with strain and of surface stress with charge in electrochemical experiments.

Contrary to experiment and computations for transition metal surfaces, which so far have invariably obtained negative-valued response to tangential strain, we find positive values for $\mathrm{d}W/\mathrm{d}e$ of Al.

Our decomposition into strain components shows that an accurate computation of $\mathrm{d}W/\mathrm{d}e$ on any surface requires that the transverse contraction is modelled. By contrast, the impact of the tangential strain on the surface relaxations is not pronounced, except for the open (110) surface.

We have inspected separately the variation of the surface dipole with strain and the strain-dependent Fermi energy. The net response parameter emerges as the small difference between the larger and nearly identical values of these contributions.

Based on an analysis of the dependence of the strain response on the electron density within the framework of the jellium model, our study links the unusual positive sign of the response of the work function to tangential strain for aluminium to its high electron density. Yet, the pronounced variation of the response with surface orientation also shows that the response behaviour cannot be understood based on the electron density alone.

Acknowledgments

We gratefully acknowledge computing resources from the German super-computing alliance HLRN.

References

[1] Ibach H 1997 *Surf. Sci. Rep.* **29** 195–263
[2] Haiss W 2001 *Rep. Prog. Phys.* **64** 591
[3] Weissmüller J, Viswanath R N, Kramer D, Zimmer P, Würschum R and Gleiter H 2003 *Science* **300** 312–5
[4] Jin H J, Wang X L, Parida S, Wang K, Seo M and Weissmüller J 2010 *Nano Lett.* **10** 187–94
[5] Detsi E, Punzhin S, Rao J, Onck P R and De Hosson J T M 2012 *ACS Nano* **6**, 3734–44
[6] Gokhshtein A Y 1969 *Doklady Akademii Nauk SSSR* **187** 601
[7] Gokhshtein A Y 1970 *Electrochim. Acta* **15** 219
[8] Gokhshtein A 1976 *Surface Tension of Solids and Adsorption* (Moscow: Nauka)
[9] Haiss W, Nichols R J, Sass J K and Charle K P 1998 *J. Electroanal. Chem.* **452** 199–202
[10] Mavrikakis M, Hammer B, and Nørskov J K 1998 *Phys. Rev. Lett.* **81** 2819–22
[11] Mavrikakis M, Stoltze P and Nørskov J 1999 *Catal. Lett.* **64** 101–6
[12] Kibler L A, El-Aziz A M, Hoyer R and Kolb D M 2005 *Angew. Chem., Int. Ed.* **44** 2080–84
[13] Tabard-Cossa V, Godin M, Burgess I J, Monga T, Lennox, R B and Grütter P 2007 *Anal. Chem.* **79** 8136–43
[14] Smetanin M, Viswanath D, Kramer D, Beckmann D, Koch T, Kibler L, Kolb D and Weissmüller J 2008 *Langmuir* **24** 8561–67
[15] Smetanin M, Kramer D, Mohanan S, Herr U and Weissmüller J 2009 *Phys. Chem. Chem. Phys.* **11** 9008–12
[16] Trassatti S 1971 *J. Electroanal. Chem.* **33** 351–78
[17] Rath D and Kolb D 1981 *Surf. Sci.* **109** 641–7
[18] Umeno Y, Elsässer C, Meyer B, Gumbsch P, Nothacker M, Weissmüller J and Evers F 2007 *Europhys. Lett.* **78** 13001
[19] Ibach H 1999 *Electrochim. Acta* **45** 575–81
[20] Viswanath R, Kramer D and Weissmüller J 2005 *Langmuir* **21** 4604–09
[21] Viswanath R N, Kramer D and Weissmüller J 2008 *Electrochim. Acta* **53** 2757–67
[22] Sekiba D, Yoshimoto Y, Nakatsuji K, Takagi Y, Iimori T, Doi S and Komori F 2007 *Phys. Rev.* B **75** 115404
[23] Albina J-M, Elsässer C, Weissmüller J, Gumbsch P and Umeno Y 2012 *Phys. Rev.* B **85** 125118
[24] Weigend F, Evers F and Weissmüller J 2006 *Small* **2** 1497–503
[25] Ibach H 2006 *Physics of Surfaces and Interfaces* (Springer)
[26] Levitin V and Loskutov S 2009 *Strained metallic surfaces: theory, nanostructuring and fatigue strength* (Weinheim: WILEY-VCH)
[27] Li W and Li D Y 2006 *J. Appl. Phys.* **99** 073502
[28] Kiejna A and Pogosov V V 2000 *Phys. Rev.* B **62** 10445
[29] Pogosov V V and Kurbatsky V P 2001 *Sov. Phys.–JETP* **92** 304–11
[30] Kresse G and Hafner J 1993 *Phys. Rev.* B **47** RC558
[31] Kresse G and Hafner J 1994 *Phys. Rev.* B **49** 14251
[32] Kresse G and Furthmüller J 1996 *Comp. Mat. Sci.* **6** 15–50
[33] Kresse G and Furthmüller J 1996 *Phys. Rev.* B **54** 11169
[34] Blöchl P E 1994 *Phys. Rev.* B **50** 17953
[35] Kresse G and Joubert D 1999 *Phys. Rev.* B **59** 1758
[36] Methfessel M and Paxton A T 1989 *Phys. Rev.* B **40** 3616
[37] Perdew J P, Burke K and Ernzerhof M 1996 *Phys. Rev. Lett.* **77** 3865–68
[38] Perdew J P, Chevary J A, Vosko S H, Jackson K A, Pederson M R, Singh D J and Fiolhais C 1992 *Phys. Rev.* B **46** 6671
[39] Perdew J P and Zunger A 1981 *Phys. Rev.* B **23** 5048
[40] Monkhorst H J and Pack J D 1976 *Phys. Rev.* B **13** 5188
[41] Fall C J, Binggeli N and Baldereschi A 1999 *J. Phys.: Condens. Matter* **11** 2689
[42] Giannozzi P *et al.* 2009 *J. Phys.: Condens. Matter* **21** 395502
[43] Finnis M W and Heine V 1974 *J. Phys. F: Met. Phys.* **4** L37
[44] Da Silva J L F 2005 *Phys. Rev.* B **71** 195416
[45] Petersen J H, Mikkelsen A, Nielsen M M and Adams D L 1999 *Phys. Rev.* B **60** 5963
[46] Stampfl C, Scheffler M, Over H, Burchhardt J, Nielsen M, Adams D L and Moritz W 1994 *Phys. Rev.* B **49** 4959
[47] Nielsen H B, Andersen J N, Petersen L and Adams D L 1982 *J. Phys. C: Solid State Phys.* **15** L1113

[48] Grepstad J, Gartland P and Slagsvold B, 1976 *Surf. Sci.* **57** 348–62
[49] Payne M C, Roberts N, Needs R J, Needels M and Joannopoulos J D 1989 *Surf. Sci.* **211-212** 1–20
[50] Smoluchowski R 1941 *Phys. Rev.* **60** 661–74
[51] Jin H-J, Parida S, Kramer D and Weissmüller J 2008 *Surf. Sci.* **602** 3588–94
[52] Deng Q, Smetanin M and Weissmüller J 2012 *ECS Meeting Abstracts* **MA2012-01** 959
[53] Wang X F, Lin J G and Xiao Y 2010 *Europhys. Lett.* **89** 66004
[54] Lang N D and Kohn W 1971 *Phys. Rev.* B **3** 1215
[55] Perdew J P, Tran H Q and Smith E D 1990 *Phys. Rev.* B **42** 11627
[56] Shore H B and Rose J H 1991 *Phys. Rev. Lett.* **66** 2519–22
[57] Rose J H and Shore H B 1991 *Phys. Rev.* B **43**, 11605
[58] Fiolhais C and Perdew J P *Phys. Rev.* B **45** 6207